Toxicology Letters 371 (2022) 9–16

Contents lists available at ScienceDirect

Toxicology Letters

journal homepage: www.journals.elsevier.com/toxicology-letters

Favipiravir induces oxidative stress and genotoxicity in cardiac and skin cells

Aysenur Gunaydin-Akyildiz [a,*,1], Nergis Aksoy [a], Tugce Boran [b], Emine Nihan Ilhan [a], Gul Ozhan [b]

[a] Bezmialem Vakif University, Faculty of Pharmacy, Department of Pharmaceutical Toxicology, 34093 Istanbul, Turkey
[b] Istanbul University, Faculty of Pharmacy, Department of Pharmaceutical Toxicology, 34116 Istanbul, Turkey

ARTICLE INFO

Editor: Angela Mally

Keywords:
Favipiravir
Oxidative stress
DNA damage
Genotoxicity
Cardiotoxicity
Dermal toxicity
Mitochondrial toxicity

ABSTRACT

Favipiravir (T-705), used against influenza viruses, is approved for emergency use in many countries for the treatment of COVID-19. The frequent adverse effects of favipiravir are related with the gastrointestinal system, however, studies suggest a positive association of favipiravir on QTc prolongation, which can cause cardiotoxicity. Also, there are reports of skin reactions such as angioedema due to favipiravir. Despite the several adverse effects, studies examining the drug's effects at the molecular level are insufficient, e.g., the genotoxic and oxidative stress-inducing effects of favipiravir, which are among the primary mechanisms of drug-induced toxicity. The cytotoxicity of favipiravir was analyzed with the measurement of the ATP content in H9c2 cardiomyoblasts and CCD-1079Sk skin fibroblasts. The ATP level decreased starting from 200 μM. The inhibitory effect on the mitochondrial electron transport chain enzymes complex I and complex V was also evaluated where favipiravir showed significant enzyme inhibitory effects in the highest concentration studied. A molecular docking study evaluating the interaction between favipiravir-RTP and mitochondrial DNA polymerase (POLG1) was done. The relationship of favipiravir with oxidative stress was examined by measuring glutathione (GSH) and protein carbonyl levels which were observed higher after drug treatment compared to the control group. The genotoxicity study was done using the Comet assay and increase in DNA tail has been detected. Furthermore, 8-OHdG levels were measured higher in favipiravir treated cells indicating oxidative DNA damage. Favipiravir induced oxidative stress leading to DNA damage in cardiomyoblast cells and fibroblastic skin cells. Oxidative stress and DNA damage might eventually lead to organ-specific damage such as cardiotoxicity and dermal toxicity. Considering the increased use of favipiravir in recent years, and that oxidative stress and genotoxicity are two important indicators of drug-induced toxicity, the obtained results are worth attention.

1. Introduction

Favipiravir (T-705) is an antiviral drug approved in 2014 by the Pharmaceuticals and Medical Devices Agency (PMDA) in Japan against influenza viruses. In addition to showing antiviral activity against resistant influenza viruses, favipiravir inhibits the replication of RNA viruses which makes it an effective treatment alternative for COVID-19 (Delang et al., 2014; Rocha-Pereira et al., 2012). As a prodrug that is converted intracellularly to the ribofuranosyl 5′-triphosphate metabolite (Favipiravir-RTP), it functions as a purine analogue having higher affinity to viral RNA-dependent RNA polymerase (RNA-dependent RNA polymerase-RdRp) than guanosine triphosphate (GTP) (Jin et al., 2013). As a chain terminator, favipiravir inhibits viral RdRp by terminating elongation at the junctional site (Sangawa et al., 2013).

Favipiravir is one of the repurposed drugs for the treatment of COVID-19. While there are several clinical studies investigating the drug's effects (clinicaltrials.gov), many countries such as Japan, Russia, Turkey and India have included favipiravir in their treatment protocol. The studies in healthy volunteers have shown that favipiravir has a C_{max} of 51.5 μg/ml (328 μM), T_{max} of 2 h and a half-life of 2–5.5 h (Madelain et al., 2016). The favipiravir dosing regimen is different in different viral infections. To achieve drug efficacy, the administered doses are indeed quite high. The approved dosing regimen for influenza virus is 2 × 1600 mg loading dose on the first day followed by 2 × 600 mg. The dosing

* Corresponding author.
E-mail address: agunaydinakyildiz@bezmialem.edu.tr (A. Gunaydin-Akyildiz).
[1] https://orcid.org/0000-0003-1196-9530

https://doi.org/10.1016/j.toxlet.2022.09.011
Received 22 June 2022; Received in revised form 7 September 2022; Accepted 20 September 2022
Available online 22 September 2022

regimen for COVID-19 is a loading dose on day 1 as 2 × 1800 mg, followed by 2 × 800 mg for 14 days (Joshi et al., 2021).

In previous clinical studies, it was concluded that the common adverse events of favipiravir are related with the gastrointestinal system and increase in the levels of uric acid and hepatic enzymes (Joshi et al., 2021). Although serious adverse events are not very likely, some pharmacodynamic studies suggest a positive association of favipiravir on QTc prolongation, which can lead to cardiotoxicity (Agrawal et al., 2020). Additionally, there are reports of sinus bradycardia and adverse skin reactions such as angioedema due to favipiravir (Islamoglu et al., 2022; Punyaratabandhu and Vanitchpongphan, 2022; Szigeti, 2022). The molecular effects of favipiravir, which may potentially lead to organ-specific damage such as cardiotoxicity and dermal toxicity, are not fully evaluated.

Oxidative stress and genotoxicity are two important aspects of drug-induced toxicity evaluation studies. Oxidative stress is the deterioration of the balance between the free radicals formed in the organism and the antioxidant defense mechanism, towards the increase of free radicals (Lobo et al., 2010). In cases where this balanced function is disturbed, a series of pathological events may occur due to oxidative stress (Uttara et al., 2009). Genotoxicity is the term that covers damages such as DNA attachments, DNA breaks, gene mutations, chromosomal abnormalities, and aneuploidy that occur in the nucleus, chromosome, and DNA structure. Genotoxic substances interact with DNA or enzymes that make copies of the genome and cause mutations (Choy, 2001; Mortelmans and Zeiger, 2000; Zeiger, 2004). Drug-induced genotoxicity has an essential role in a series of pathological events. The studies about the potential genotoxic effects of favipiravir along with its relationship with oxidative stress are lacking.

In this study, the molecular effects of favipiravir were evaluated using the H9c2 cardiomyoblasts and CCD-1079Sk skin fibroblasts in aspects of oxidative stress and genotoxicity. Oxidative stress and DNA damage may eventually lead to organ-specific damage such as cardiotoxicity and dermal toxicity. Understanding favipiravir's adverse effects at the molecular level will provide insight to minimizing them for protecting patients from drug-induced adverse effects. Considering the wide use of favipiravir in the past three years, and the lack of studies examining the drug's effects at the molecular level, such detailed molecular studies are of quite importance.

2. Materials and methods

2.1. Cell culture

Rat cardiomyoblasts H9c2 (CRL-1446™) and human skin fibroblasts CCD-1079Sk (CRL-2097™) were purchased from American Type Culture Collection (ATCC, VA, USA), and cultured in DMEM-F12 medium supplemented with 10% fetal bovine serum and 1 % penicillin–streptomycin (Gibco, USA). Sub-culturing was done every 2–3 days.

2.2. Favipiravir treatment

Favipiravir was purchased from Selleckchem (USA) and dissolved in DMSO. The studied concentrations were chosen according to the ATP assay, the cytotoxicity assay, which was done in the range of 100–500 μM. Under the cell culture conditions, it was possible to study 500 μM as the maximum studied concentration, at which the cell viability inhibition was < %20. The ATP level decreased starting from 200 μM. Therefore, 200 μM and 400 μM were selected for the genotoxicity and oxidative stress analysis. For the in vitro enzyme inhibition assays (complex I and complex V) the favipiravir concentration range was 25–800 μM. All studied concentration ranges cover the clinical Cmax level of favipiravir (328 μM). The control group was the solvent containing the same percentage of DMSO (0.1 %) with the treatment groups.

2.3. ATP bioluminescence assay

ATP content of the cells was determined with recording the bioluminescence using CellTiter-Glo® 2.0 (Promega, USA). The luminescent signal is proportional to the ATP content of the cells which is an indicator of cell viability (Hannah et al., 2001). Opaque white 96-well plates were used. H9c2 and CCD-1079Sk cells were seeded 10^4/well and favipiravir treatment was conducted after a 24 h incubation. Following 24 h favipiravir treatment, the cells were shaken for 2 min with CellTiter-Glo® 2.0 Reagent equal to the volume of cell culture medium present in each well. Then the plate was incubated for 10 min in room temperature to stabilize the luminescence signal. Finally, the luminescence was recorded using a BioTek Synergy H1 (Epoch, Germany) microplate reader. The results are given as a percentage relative to the solvent control group.

2.4. Mitochondrial electron transport chain enzyme activity assay

The effects of favipiravir on complex I and complex V were evaluated using the MitoTox™ Complex I OXPHOS Activity Assay Kit (ab109903-Abcam, UK) and MitoTox™ Complex V OXPHOS Activity Assay Kit (ab109907-Abcam, UK) following the manufacturer's instructions. The oxidative phosphorylation enzymes actively play role in mitochondrial ATP production.

2.5. Protein carbonyl assay

For determining the levels of protein carbonyl as an indicator of oxidative stress, protein carbonyl enzyme-linked immunosorbent (ELISA) assay kit (Bioassay Technology Laboratory, China) has been used. According to the kit description, briefly, the cells were seeded in T-25 flasks. After 24 h, favipiravir treatment was conducted, and the cells were incubated for another 24 h and collected by trypsinization into centrifuge tubes. The supernatant formed after centrifugation was discarded and the precipitate was dispersed in PBS. The newly formed mixture was centrifuged, and the supernatant formed after centrifugation was discarded and the precipitate was again dispersed in PBS. The cell PBS mixtures were freeze-thawed three times. Then, it was centrifuged again, and the supernatant obtained as a result of centrifugation was used during the experiment according to the kit description. The protein carbonyl level of cells was measured at 450 nm using a BioTek Synergy H1 microplate reader. The protein concentrations were measured using the BCA Protein Assay kit (Intron Biotechnology, Korea) and the results are given as ng/mg protein.

2.6. Glutathione (GSH) detection

GSH detection was done using the method described by Beutler (1975) which is based on 5,5′-Dithiobis-2-nitrobenzoic acid (DTNB) reaction with free sulfhydryl groups giving yellow colored 2-nitro-5 mercaptobenzoic acid. The reaction mixture contained 200 μL of 10.000 g supernatant or standard, 800 μL seconder sodium phosphate buffer and 100 μL DTNB (Sigma-Aldrich, St.Louis, MO, USA). After vortex and 5 min incubation at room temperature, the absorbance was measured by spectrophotometry at 412 nm using a BioTek Synergy H1 microplate reader. The protein concentrations were measured using the BCA Protein Assay kit (Intron Biotechnology, Korea) and the results are given as ng/mg protein.

2.7. Comet assay

Genotoxicity (DNA damage) evaluation was done using the alkaline Comet assay method. The cells were seeded in T-25 flasks and were incubated for 24 h for adherence to the plate. Favipiravir treatment was conducted, and the cells were collected after 24 h treatment. The supernatant formed after centrifugation was discarded and the precipitate

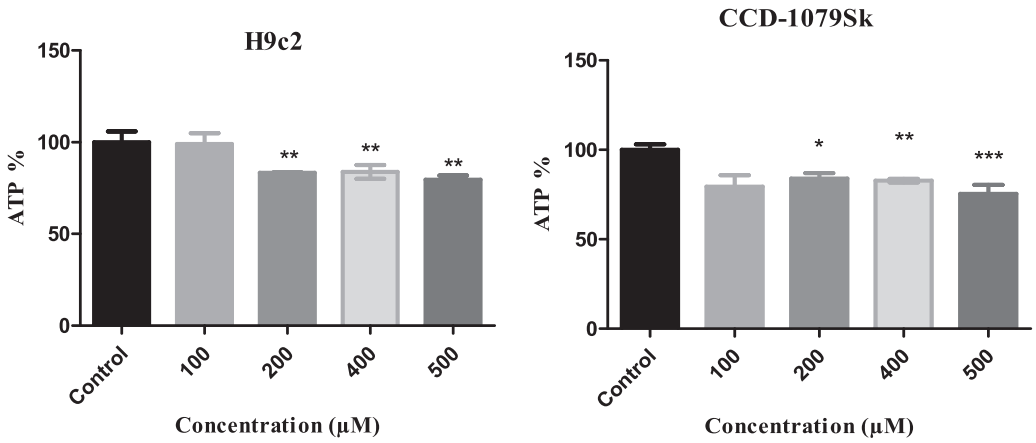

Fig. 1. Effects of favipiravir on the ATP content of H9c2 and CCD-1079Sk cells after 24 h treatment. The cells were treated with 100–500 µM concentrations. Data are expressed as mean ± SD, * $p < 0.05$ ** $p < 0.01$ and *** $p < 0.001$ versus the control group.

was dispersed in PBS. Slides previously coated with agarose were used to spread the cells. 100 µL of the sample was mixed with 100 µL of 0.65% low melting agarose, spread on a slide and covered with a coverslip. After the slides were kept in + 4 °C, the coverslips were removed and immersed in the lysis solution (10 mM Tris, 2.5 M NaCl, 100 mM EDTA, distilled water) and kept in this state for 1 h at + 4 °C. The slides were placed in the electrophoresis tank. The electrophoresis tank was filled with alkaline electrophoresis solution (3 % NaOH, 0.5 %EDTA) and set to 25 V 300 mA for 20 min and electrophoresis was started. After the electrophoresis was finished, the slides were kept in neutralizer buffer (0.4 M Tris) for 20 min. After the slides were removed from the neutralizer buffer, the slides were stained with ethidium bromide solution (100 µg/ml) and were examined under a microscope. The DNA damage was assessed from the percentage of DNA in the tail (TI %). One hundred cells were assessed per slide using a Comet assay IV image analysis system (Perceptive Instruments, UK). 50 µM H_2O_2 was used as a positive control.

2.8. 8-Hydroxy-2′-deoxyguanosine (8-OHdG) detection

As an indicator of oxidative stress-induced DNA damage, the quantitative level of 8-OHdG was detected using an ELISA kit (AFG Scientific, USA) according to the manufacturer's manuel. Briefly, the cells were seeded in T-25 flasks and were incubated for 24 h for adherence to the plate. Favipiravir treatment was conducted, and the cells were collected after 24 h treatment. The supernatant formed after centrifugation was discarded and the precipitate was dispersed in PBS. After repeated freeze-thaw cycles, a 20-minute centrifugation at 3000 rpm was done and the supernatant was collected to be used during the experiment according to the kit description. The 8-OHdG level of the cells was measured at 450 nm using a BioTek Synergy H1 microplate reader. The protein concentrations were measured using the BCA Protein Assay kit (Intron Biotechnology, Korea) and the results are given as ng/mg protein.

2.9. Molecular docking study

The crystal structure of POLG1 complexed with its inhibitor zalcitabine-triphosphate at 3.44 Å resolution (PDB ID: 4ZTZ) was retrieved from the RCSB Protein Data Bank. The docking study was carried out using the Schrödinger Software Suite (Maestro Schrödinger Release 2022, NY, 2022). The crystal structures of the enzymes were prepared using the Protein Preparation Wizard Module of Schrödinger Software Suite (Sastry, 2013). The retrieved crystal structure was optimized by removing water molecules, heteroatoms, and co-factors. The hydrogens, missing atoms, bonds, and charges were computed and corrected through Maestro. The studied compounds and the co-crystallized ligand zalcitabine were also prepared and optimized (generating various tautomers and ring conformations, assigning bond orders, and stereochemistries) using the LigPrep module. All the conformations generated were minimized using the OPLS4 forcefield. The receptor grid was generated around the co-crystalized ligand of the enzyme to specify the binding site, where the grid box size was determined with the receptor Grid Generation implemented in Glide.

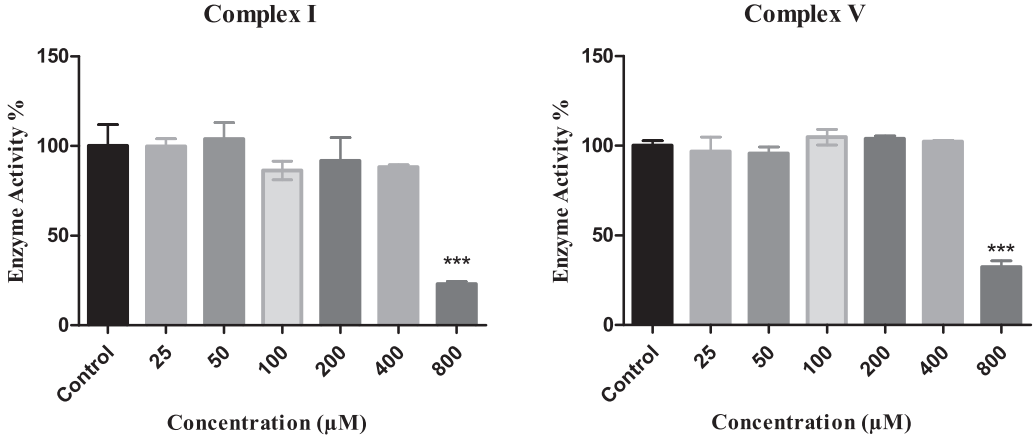

Fig. 2. Dose-dependent effect of favipiravir on mitochondrial complex I and complex V enzyme activities. Data are expressed as mean ± SD, *** $p < 0.001$ versus the control group.

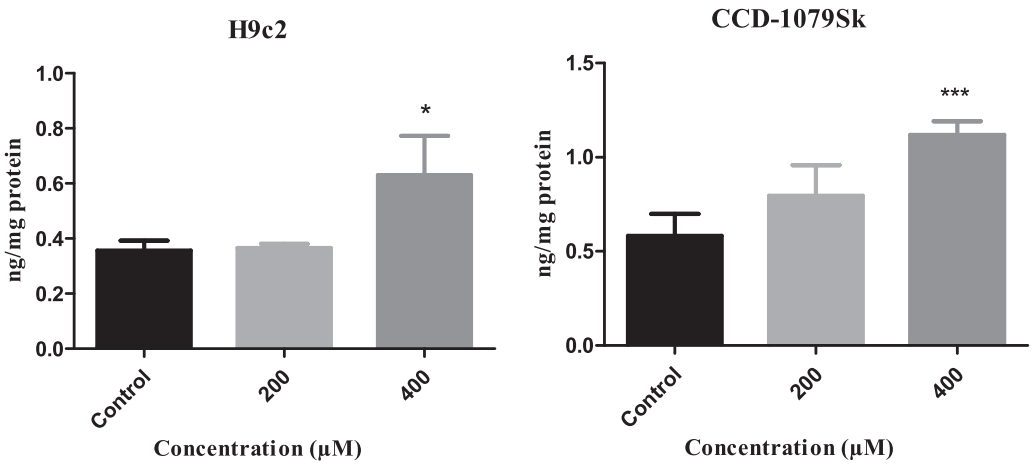

Fig. 3. Effect of favipiravir on protein carbonyl level of the H9c2 and CCD-1079Sk cells following 24 h treatment. The cells were treated with 200 µM and 400 µM favipiravir for 24 h. Data are expressed as mean ± SD, *** $p < 0.001$ versus the control group.

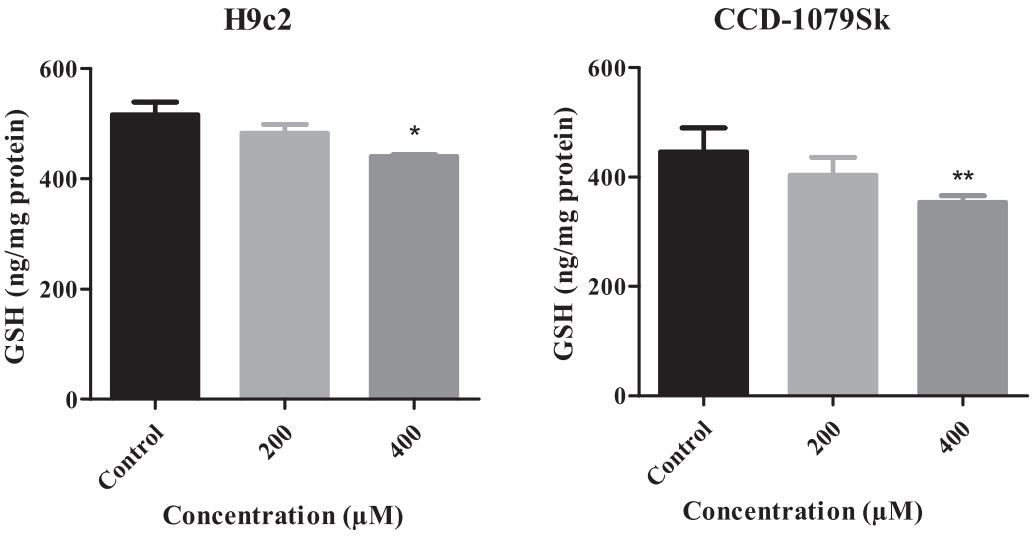

Fig. 4. Effect of favipiravir on the GSH level of the H9c2 and CCD-1079Sk cells following 24 h treatment. The cells were treated with 200 µM and 400 µM favipiravir for 24 h. Data are expressed as mean ± SD, *p < 0.05, ** $p < 0.01$ versus the control group.

Zalcitabine, the native ligand, is similar to favipiravir in terms of activity, thus, grid-box was created with a focus on zalcitabine co-crystallized ligand as a pharmacophoric site. The Glide docking was performed in the Standard Precision (SP) mode for 4ZTZ (Friesner et al., 2004; Friesner et al., 2006; Halgren et al., 2004).

2.10. Statistical analysis

Statistical analysis was performed using Graphpad Prism 6. Statistical differences were evaluated with one-way ANOVA followed by the Tukey test. The results were represented as mean ± standard deviation (SD).

3. Results

3.1. Intracellular ATP content

Significant 20 % decrease in ATP content was observed at 200, 400 and 500 µM concentrations after 24 h of favipiravir treatment in the H9c2 cell line (Fig. 1). A similar inhibition was seen in the CCD-1079Sk cell line after treatment with all the concentrations studied. The ATP content of the cells indicates cell viability.

3.2. Mitochondrial electron transport chain enzyme activity assay

The enzyme inhibitory effect of favipiravir was analyzed to for evaluating the mitochondrial ATP synthesizing enzyme activities. The activity of complex I was observed to decrease starting from 100 µM, and significantly inhibited at the highest concentration (800 µM). Similarly, complex V activity was significantly inhibited at 800 µM (Fig. 2).

3.3. Protein carbonyl level

According to the cell viability results (−20 % ATP) 200 µM and 400 µM concentrations of favipiravir was chosen for treating the cells for evaluating the protein carbonyl levels. The protein carbonyl level after exposure to favipiravir significantly increased in the 400 µM concentration treatment group in both cell lines (Fig. 3). Oxidative stress is proportional to the formation of protein carbonyl.

3.4. GSH level

The GSH levels of the cells after 200 and 400 µM concentrations of favipiravir for 24 h are given in Fig. 4. The inhibition of the GSH levels is

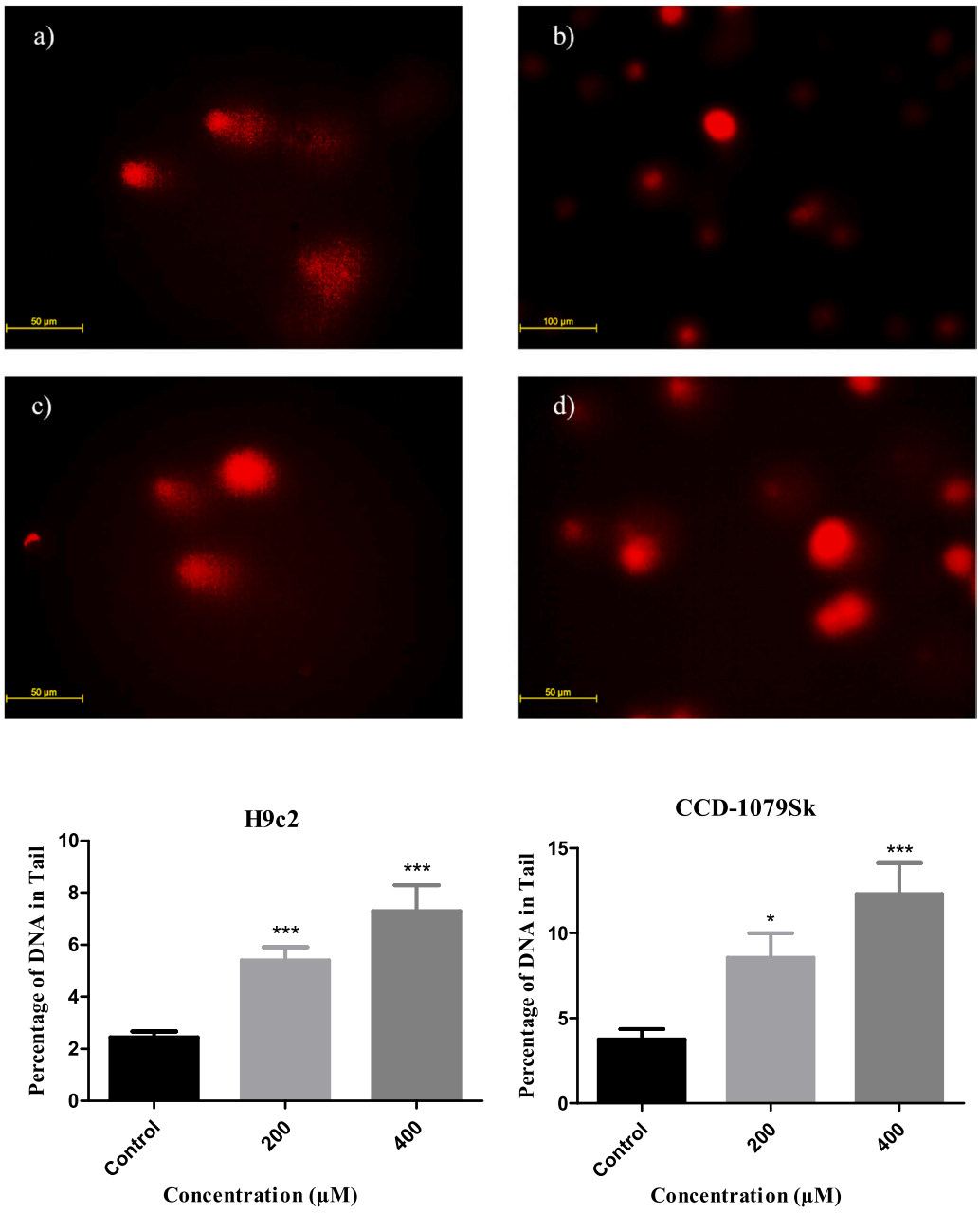

Fig. 5. Alkaline Comet assay results of H9c2 and CCD-1079Sk cells treated with 200 µM and 400 µM concentrations of favipiravir for 24 h. a) Image of H9c2 DNA after 400 µM favipiravir treatment. b) Image of H9c2 DNA control group. c) Image of CCD-1079Sk DNA after 400 µM favipiravir treatment. d) Image of CCD-1079Sk DNA control group. Data are expressed as mean ± SEM, * $p < 0.05$ and * ** $p < 0.001$ versus the control group.

a sign of the decrease of the antioxidant capacity of the cells making them more vulnerable to oxidative stress.

3.5. Comet assay

The genotoxicity results measured by the Comet assay after 200 and 400 µM concentrations of favipiravir for 24 h are given in Fig. 5. Genotoxicity is proportional to the length of the DNA in the tail.

3.6. 8-OHdG level

The genotoxicity results by the 8-OHdG measurement after 200 and 400 µM concentrations of favipiravir for 24 h are given in Fig. 6. The quantitative amount of 8-OHdG is an indicator of DNA damage.

3.7. Molecular docking of favipiravir-RTP with mitochondrial DNA polymerase subunit gamma-1 (POLG1)

Favipiravir-RTP and its interactions with the binding site of 4ZTZ are given in Fig. 7. and Table 1. The docking score was determined as − 8.483 kcal/mol. In the active site of the receptor, favipiravir-RTP is surrounded with ARG943, GLU1136, LYS925, LYS947, TYR951 amino acid residues, along with MG4001, MG4002. There are hydrogen bonds between the amin group and GLU1136, oxygen of a phosphate group and LYS 947 and ARG943, oxygen of a phosphate group and TYR951. The pyrazine ring forms a pi cation interaction with LYS947 which has multiple salt bridges with the phosphate groups. Furthermore, the phosphate groups have multiple salt bridges and metal coordination with MG4001 and MG4002. The validation was done for the docking model and the Root mean square (RMS) value was found 0.733 by

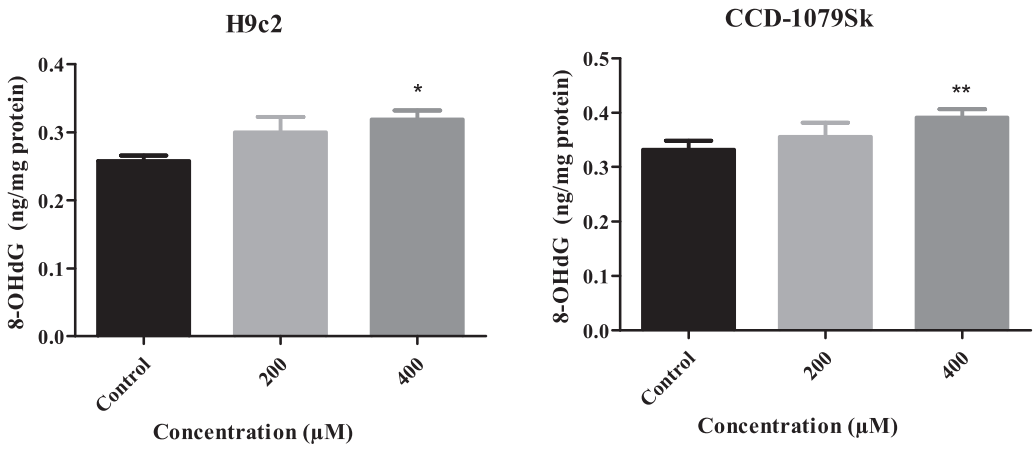

Fig. 6. Effect of favipiravir on 8-OHdG of the H9c2 and CCD-1079Sk cells following 24 h treatment. The cells were treated with 200 µM and 400 µM favipiravir for 24 h. Data are expressed as mean ± SD, *p < 0.05, ** $p < 0.01$ versus the control group.

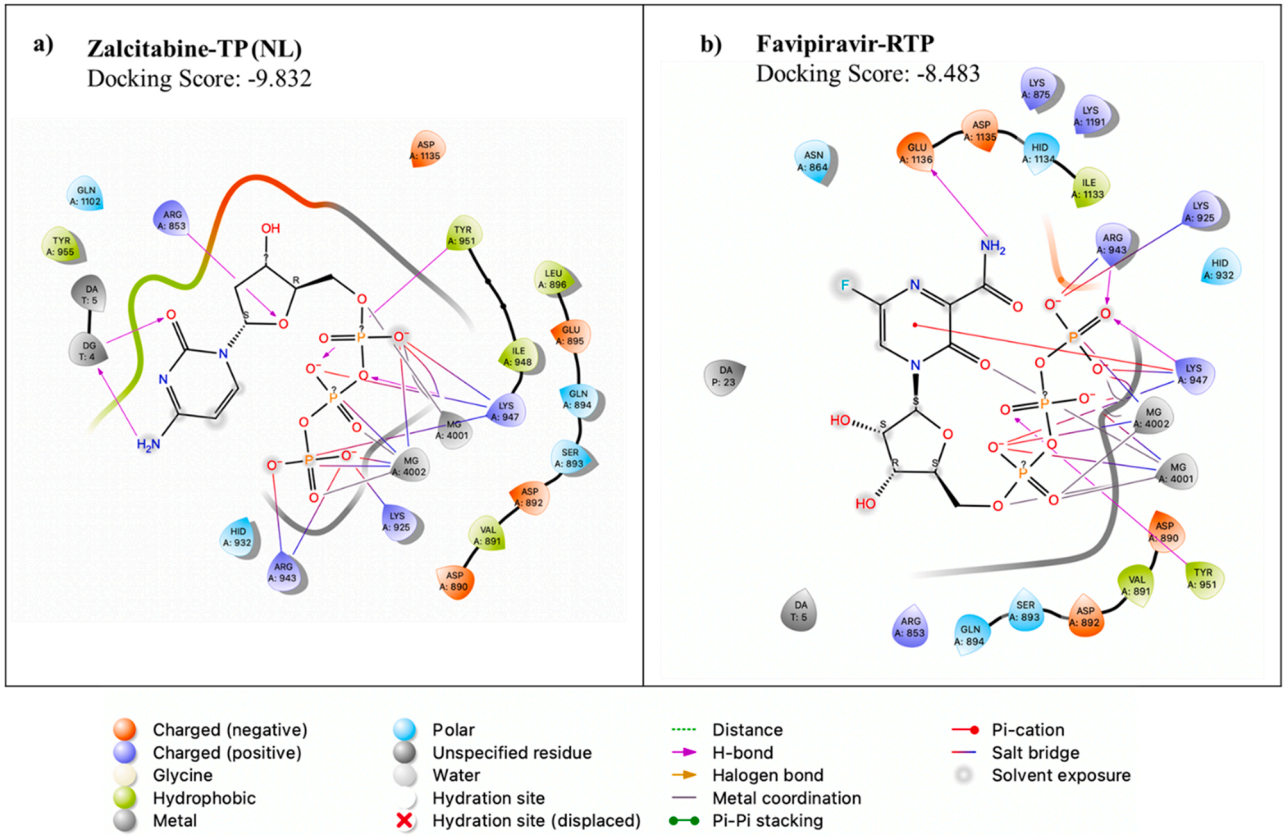

Fig. 7. Zalcitabine-TP (a) and Favipiravir-RTP (b) and their 2D interactions with the active site of the crystal structure of POLG1 (PDB ID: 4ZTZ). NL: Native ligand.

superpositioning the docked pose and experimental binding conformation of Zalcitabine-TP in the binding pocket of 4ZTZ.

4. Discussion

Favipiravir, which was approved for emergency use in many countries during the COVID-19, and millions of people have been prescribed since the beginning of the pandemic. Clinical trials are ongoing in Japan, China, the USA, India, Saudi Arabia, etc. (clinicaltrials.gov). There is a lack of knowledge about the side effects of favipiravir, especially at the molecular level. The aim of our study was to examine whether favipiravir induced cytotoxicity, genotoxicity, and/or oxidative damage using the cardiomyoblastic cell line H9c2 and the skin fibroblastic cell line CCD-1079Sk. Toxicity at the cellular level can lead to organ-specific damage such as cardiotoxicity and dermal toxicity.

The effect of favipiravir on QTc prolongation is unclear, with some pharmacodynamic studies suggesting a positive association (Agrawal et al., 2020). Computational studies about the effects of favipiravir on the human ether-a-go-go gene (hERG) block have shown that a mild suppression of the hERG current was observed at the concentration of 1 mM (Michaud et al., 2021). They also stated in the study that; "*As no reports of drug-induced long QT syndrome have been published yet, close monitoring of QTc remains advisable.*". Favipiravir-induced chest pain has been reported (Ivashchenko et al., 2020), and a recent report presents

Table 1
The docking scores and interactions with the active site of POLG1 crystal structure (PDB ID:4ZTZ).

Ligand	Docking Score (kcal/mol)	H-bond	Pi-cation	Salt bridge	Metal Coordination
Zalcitabine-TP (Native Ligand)	-9.832	ARG853 TYR951 LYS947	–	ARG943 LYS925 LYS947 MG4001 MG4002	MG4001 MG4002
Favipiravir-RTP	-8.483	GLU1136 ARG943 LYS947 TYR951	LYS947	ARG943 LYS925 LYS947 MG4001 MG4002	MG4001 MG4002

sinus bradycardia as a potential side effect of favipiravir (Szigeti, 2022). However, favipiravir had negligible effects when assessed for proarrhythmic risk and contraction impairment in human-induced pluripotent stem cell-derived cardiomyocytes (Yanagida et al., 2021). Five cases of cutaneous skin reactions were reported after favipiravir treatment in COVID-19 patients (Punyaratabandhu & Vanitchpongphan, 2022). Recently, two cases of angioedema were reported due to favipiravir (Islamoglu et al., 2022). The reports published since favipiravir was used widely in the past 3 years, about the drug's adverse effects were mainly on cardiotoxicity and dermal toxicity. Therefore, the cardiomyoblastic cell line H9c2 and skin fibroblasts CCD-1079Sk were seen reasonable to investigate favipiravir's adverse effects in this study.

According to the results of our present study, favipiravir does not show high cytotoxicity to neither cell lines, which was also confirmed with different studies in the literature with different mammalian cell lines (Furuta et al., 2002). Despite its low cytotoxicity, the ATP level was seen to be inhibited starting from 200 μM. ATP depletion may be a sign of cellular stress. Oxidative phosphorylation in the mitochondria provides ATP synthesis therefore evaluating the electron transport chain enzymes activities may help to explain the inhibition of the ATP levels observed after favipiravir treatment. Complex V (ATP-synthase, the primary enzyme responsible for synthesizing ATP) was observed to be inhibited in the highest favipiravir concentration, while complex I was seen to be inhibited starting from 100 μM.

The molecular docking study of the interaction between favipiravir-RTP and DNA polymerase gamma (POLG1), an enzyme responsible for mitochondrial DNA replication, which is susceptible to inhibition by dideoxynucleoside-based inhibitors such as zalcitabine (Szymanski et al., 2015). In the conducted molecular docking study to evaluate favipiravir-RTP's interaction with POLG1, it was seen that favipiravir has notable interactions giving a high docking score which is close to the docking score of the positive control zalcitabine-TP. These results may be useful to evaluate further drug-induced mitochondrial toxicity and examining heart mitochondria after favipiravir treatment in vivo could be a reasonable approach for it. The mitochondrial cardiotoxicity of nucleoside analogue reverse transcriptase inhibitors has been studied in detail and such studies reveal that these antiviral drugs cause oxidative stress and mitochondrial DNA damage potentially leading to cardiotoxicity (Lewis et al., 2003). The mechanism of action of favipiravir is similar to these drugs and oxidative stress is an important parameter to evaluate.

The antioxidant GSH levels of the cells were observed to decrease after favipiravir treatment. GSH is an antioxidant and oxidative stress occurs with the deterioration of the balance between the free radicals formed in the organism and the antioxidant defense mechanism, towards the increase of free radicals (Lobo et al., 2010). In cases where this balanced function is disturbed, a series of pathological events may occur due to oxidative stress (Uttara et al., 2009). The protein carbonylation levels which are bioindicators of oxidative stress (Suzuki et al., 2010)

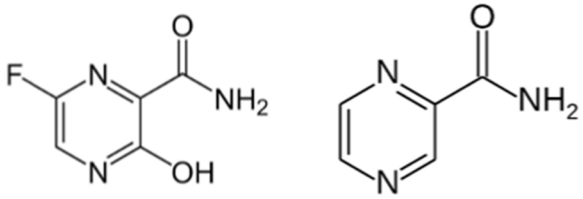

Fig. 8. Chemical structures of favipiravir (left) and pyrazinamide (right).

were observed significantly higher in favipiravir treated cells. Zalcitabine was previously shown to increase protein carbonyl levels and lipid peroxidation indicating oxidative stress (Opii et al., 2007). Taking these results into account, favipiravir seems to induce oxidative stress in the cells.

This may also be an underlying factor of the drug's unknown potential genotoxic profile since an important consequence of oxidative stress is DNA damage (Gonzalez-Hunt et al., 2018). In nuclear and mitochondrial DNA, 8-hydroxy-2′ -deoxyguanosine (8-OHdG) is one of the predominant forms of free radical-induced oxidative lesions which is used as a biomarker for oxidative stress-induced DNA damage (Valavanidis et al., 2009). A concentration-dependent increase was observed in the quantitative analysis of 8-OHdG after favipiravir treatment in our study indicating possible oxidative DNA damage. A comprehensive meta-analysis to explore the relationship between 8-OHdG levels and heart failure revealed that patients with heart failure had higher levels of 8-OHdG compared to the controls (Di Minno et al., 2017).

Although studies on the genotoxic effects of favipiravir is lacking, it has been reported that the drug pyrazinamide, which is structurally similar to favipiravir and used in the treatment of tuberculosis, causes chromosomal abnormalities and DNA damage, and that it may be toxic at the genetic level (Sharma & Sharma, 2017). In a genotoxicity evaluation study, DNA damage was detected in the liver, kidney and blood samples taken from rats given pyrazinamide for 90 days orally by the Comet assay (Arslan et al., 2015). The molecular structure of favipiravir similar to pyrazinamide brings to mind that favipiravir may also cause DNA damage (Fig. 8). Similar to these results, our study results indicated DNA damage in the 400 μM concentration groups in both cell lines.

5. Conclusions

The aim of this study was to examine whether favipiravir induced cytotoxicity, genotoxicity, and/or oxidative damage in the H9c2 and CCD-1079Sk cell lines. The protein carbonyl and Comet assay results showed that oxidative stress and genotoxicity were evident in both cell lines. Favipiravir has an estimated C_{max} of 328 μM which is close to the concentrations in the present study. For this reason, it is important to carry out further studies to evaluate favipiravir in terms of genotoxicity and oxidative damage which are the two interrelated underlying mechanisms of drug-induced toxicity. Considering the wide use of favipiravir against RNA virus infections especially in the past three years, and the lack of studies examining the drug's effects at the molecular level, such detailed molecular studies are important to be promoted for further evaluations.

Declaration of Competing Interest

The authors declare that they have no known competing financial interests or personal relationships that could have appeared to influence the work reported in this paper.

Data Availability

Data will be made available on request.

Acknowledgments

This work was supported by the Scientific Research Projects Coordination Unit and Drug Application and Research Center (İLMER) of Bezmialem Vakif University Scientific Research Projects Unit, Turkey (Project Number: 20210208E) and The Scientific and Technological Research Council of Türkiye (TÜBİTAK), Turkey (Project Number: 1919B012003864). We thank Dr. Eray Metin Guler for his support in analyzing the results in this study. The manuscript has been read and approved by all co-authors, and there is no conflict of interest between authors of this article.

References

Agrawal, U., Raju, R., Udwadia, Z.F., 2020. Favipiravir: a new and emerging antiviral option in COVID-19. Med. J. Armed Forces India 76 (4), 370–376.
Arslan, K., Kanbur, M., Karabacak, M., Sarıca, Z., TAŞÇıOĞLU, N., İşcan, K., Dündar, M., Akçay, A., 2015. Genotoxic effects of some antituberculosis drugs and mixtures in rats. Drug Res. 65 (04), 219–222.
Choy, W.N., 2001. Genetic Toxicology and Cancer Risk Assessment. Marcel Dekker, New York.
Beutler, E., 1975. Red Cell metabolism. A Manual of Bichemical Methods, 2nd ed., 1975. Grune & Stratton, New York, pp. 71–73.
Delang, L., Segura Guerrero, N., Tas, A., Quérat, G., Pastorino, B., Froeyen, M., Dallmeier, K., Jochmans, D., Herdewijn, P., Bello, F., 2014. Mutations in the chikungunya virus non-structural proteins cause resistance to favipiravir (T-705), a broad-spectrum antiviral. J. Antimicrob. Chemother. 69 (10), 2770–2784.
Di Minno, A., Turnu, L., Porro, B., Squellerio, I., Cavalca, V., Tremoli, E., Di Minno, M.N., 2017. 8-Hydroxy-2- deoxyguanosine levels and heart failure: a systematic review and meta-analysis of the literature. Nutr. Metab. Cardiovasc. Dis. 27, 201–208.
Friesner, R.A., Banks, J.L., Murphy, R.B., Halgren, T.A., Klicic, J.J., Mainz, D.T., Repasky, M.P., Knoll, E.H., Shelley, M., Perry, J.K., 2004. Glide: a new approach for rapid, accurate docking and scoring. 1. Method and assessment of docking accuracy. J. Med. Chem. 47 (7), 1739–1749.
Friesner, R.A., Murphy, R.B., Repasky, M.P., Frye, L.L., Greenwood, J.R., Halgren, T.A., Sanschagrin, P.C., Mainz, D.T., 2006. Extra precision glide: docking and scoring incorporating a model of hydrophobic enclosure for protein− ligand complexes. J. Med. Chem. 49 (21), 6177–6196.
Furuta, Y., Takahashi, K., Fukuda, Y., Kuno, M., Kamiyama, T., Kozaki, K., Nomura, N., Egawa, H., Minami, S., Watanabe, Y., 2002. In vitro and in vivo activities of anti-influenza virus compound T-705. Antimicrob. Agents Chemother. 46 (4), 977–981.
Gonzalez-Hunt, C.P., Wadhwa, M., Sanders, L.H., 2018. DNA damage by oxidative stress: measurement strategies for two genomes. Curr. Opin. Toxicol. 7, 87–94.
Halgren, T.A., Murphy, R.B., Friesner, R.A., Beard, H.S., Frye, L.L., Pollard, W.T., Banks, J.L., 2004. Glide: a new approach for rapid, accurate docking and scoring. 2. Enrichment factors in database screening. J. Med. Chem. 47 (7), 1750–1759.
Hannah, R., Beck, M., Moravec, R., Riss, T., 2001. CellTiter-Glo™ luminescent cell viability assay: a sensitive and rapid method for determining cell viability. Promega Cell Notes 2, 11–13.
Islamoglu, M.S., Dokur, M., Uysal, B.B., Onal, B., 2022. Angioedema after favipravir treatment: two cases. J. Cosmet. Dermatol.
Ivashchenko, A.A., Dmitriev, K.A., Vostokova, N.V., Azarova, V.N., Blinow, A.A., Egorova, A.N., Gordeev, I.G., Ilin, A.P., Karapetian, R.N., Kravchenko, D.V., 2020. AVIFAVIR for treatment of patients with moderate COVID-19: interim results of a phase II/III multicenter randomized clinical trial. medRxiv.
Jin, Z., Smith, L.K., Rajwanshi, V.K., Kim, B., Deval, J., 2013. The ambiguous base-pairing and high substrate efficiency of T-705 (favipiravir) ribofuranosyl 5′-triphosphate towards influenza A virus polymerase. PLoS One 8 (7), e68347.
Joshi, S., Parkar, J., Ansari, A., Vora, A., Talwar, D., Tiwaskar, M., Patil, S., Barkate, H., 2021. Role of favipiravir in the treatment of COVID-19. Int. J. Infect. Dis. 102, 501–508.
Lewis, W., Day, B.J., Copeland, W.C., 2003. Mitochondrial toxicity of NRTI antiviral drugs: an integrated cellular perspective. Nat. Rev. Drug Discov. 2 (10), 812–822.
Lobo, V., Patil, A., Phatak, A., Chandra, N., 2010. Free radicals, antioxidants and functional foods: impact on human health. Pharmacogn. Rev. 4 (8), 118.
Madelain, V., Nguyen, T.H.T., Olivo, A., De Lamballerie, X., Guedj, J., Taburet, A.-M., Mentré, F., 2016. Ebola virus infection: review of the pharmacokinetic and pharmacodynamic properties of drugs considered for testing in human efficacy trials. Clin. Pharmacokinet. 55 (8), 907–923.
Michaud, V., Dow, P., Al Rihani, S.B., Deodhar, M., Arwood, M., Cicali, B., Turgeon, J., 2021. Risk assessment of drug-induced long QT syndrome for some COVID-19 repurposed drugs. Clin. Transl. Sci. 14 (1), 20–28.
Mortelmans, K., Zeiger, E., 2000. The ames Salmonella/microsome mutagenicity assay. Mutat. Res. /Fundam. Mol. Mech. Mutagen. 455 (1–2), 29–60.
Opii, W.O., Sultana, R., Abdul, H.M., Ansari, M.A., Nath, A., Butterfield, D.A., 2007. Oxidative stress and toxicity induced by the nucleoside reverse transcriptase inhibitor (NRTI)–2′,3′-dideoxycytidine (ddC): relevance to HIV-dementia. Exp. Neurol. 204 (1), 29–38.
Punyaratabandhu, P., Vanitchpongphan, S., 2022. Favipiravir-induced cutaneous adverse reactions in patients infected with COVID-19. Clin. Exp. Dermatol. 47 (3), 573–577.
Rocha-Pereira, J., Jochmans, D., Dallmeier, K., Leyssen, P., Nascimento, M., Neyts, J., 2012. Favipiravir (T-705) inhibits in vitro norovirus replication. Biochem. Biophys. Res. Commun. 424 (4), 777–780.
Sangawa, H., Komeno, T., Nishikawa, H., Yoshida, A., Takahashi, K., Nomura, N., Furuta, Y., 2013. Mechanism of action of T-705 ribosyl triphosphate against influenza virus RNA polymerase. Antimicrob. Agents Chemother. 57 (11), 5202–5208.
Sastry, M., 2013. Protein and ligand preparation: parameters, protocols, and influence on virtual screening enrichments (Madhavi Sastry G., Adzhigirey M., Day T., Annabhimoju R., Sherman W.). J. Comput. Aided Mol. 221–234.
Sharma, R., Sharma, V.L., 2017. Deleterious effects of 28-day oral co-administration of first-line anti-TB drugs on spleen, blood and bone marrow chromosomes in normal rat. Drug Chem. Toxicol. 40 (2), 154–163.
Suzuki, Y.J., Carini, M., Butterfield, D.A., 2010. Protein carbonylation. Antioxid. Redox Signal. 12 (3), 323–325.
Szigeti, J., 2022. Sinus bradycardia as a potential side effect of favipiravir treatment. Orv. Hetil. 163 (7), 267–270.
Szymanski, M.R., Kuznetsov, V.B., Shumate, C., Meng, Q., Lee, Y.S., Patel, G., Patel, S., Yin, Y.W., 2015. Structural basis for processivity and antiviral drug toxicity in human mitochondrial DNA replicase. EMBO J. 34 (14), 1959–1970.
Uttara, B., Singh, A.V., Zamboni, P., Mahajan, R., 2009. Oxidative stress and neurodegenerative diseases: a review of upstream and downstream antioxidant therapeutic options. Curr. Neuropharmacol. 7 (1), 65–74.
Valavanidis, A., Vlachogianni, T., Fiotakis, C., 2009. 8-hydroxy-2′ -deoxyguanosine (8-OHdG): a critical biomarker of oxidative stress and carcinogenesis. J. Environ. Sci. Health Part C Environ. Carcinog. Ecotoxicol. Rev. 27 (2), 120–139.
Yanagida, S., Satsuka, A., Hayashi, S., Ono, A., Kanda, Y., 2021. Comprehensive cardiotoxicity assessment of COVID-19 treatments using human-induced pluripotent stem cell-derived cardiomyocytes. Toxicol. Sci. 183 (1), 227–239.
Zeiger, E., 2004. History and Rationale of Genetic Toxicity Testing: An Impersonal, and Sometimes Personal View, Vol. 44. Wiley Online Library,, pp. 363–371.